Growth, geometry, and mechanics of a blooming lily

Haiyi Liang[a,b] **and L. Mahadevan**[a,1]

Engineering and Applied Sciences, Organismic and Evolutionary Biology, Wyss Institute, Kavli Institute, Harvard University, Cambridge, MA 02138; and Department of Modern Mechanics, University of Science and Technology of China—Hefei, Anhui 230026, People's Republic of China

Edited by James S. Langer, University of California, Santa Barbara, CA, and approved January 24, 2011 (received for review June 4, 2010)

Despite the common use of the blooming metaphor, its floral inspiration remains poorly understood. Here we study the physical process of blooming in the asiatic lily *Lilium casablanca*. Our observations show that the edges of the petals wrinkle as the flower opens, suggesting that differential growth drives the deployment of these laminar shell-like structures. We use a combination of surgical manipulations and quantitative measurements to confirm this hypothesis and provide a simple theory for this change in the shape of a doubly curved thin elastic shell subject to differential growth across its planform. Our experiments and theory overturn previous hypotheses that suggest that blooming is driven by differential growth of the inner layer of the petals and in the midrib by providing a qualitatively different paradigm that highlights the role of edge growth. This functional morphology suggests new biomimetic designs for deployable structures using boundary or edge actuation rather than the usual bulk or surface actuation.

mechanics | curvature reversal

Plant and fungal movements, although limited by the absence of dedicated motile elements such as muscles, are nevertheless varied. They span a range of length and time scales, from the rapid movements in microscopic nematophagous fungi (1), to the slow opening and closing of leaf stomata. A striking example of rapid movements is seen in the Venus flytrap, which snaps in a fraction of a second as a result of an actively controlled release of turgor across the thickness of the leaf, switching its curvature (2). This and other examples of rapid movements in plants and fungi usually involve slender geometries and may be quantified in terms of the motion of water flow in a soft porous solid (3). Morphological transitions that guide cell,tissue, leaf, branch, root, and stem shape, on the other hand, are much slower and are driven by differential growth. Here we consider a ubiquitous example of plant movement driven by differential growth, the blooming of a flower, the inspiration for much art and poetry but surprisingly little science.

When a flower blossoms, its petals change curvature on a time scale of a few hours to days, consistent with the idea that these movements are growth driven. In flowers that bloom just once, differential cell proliferation is the dominant mode of growth, whereas in those that open and close repeatedly, cell elongation plays an important role (4). Frequently proposed explanations for petal movements posit a difference in growth rate between the abaxial and adaxial sides (surfaces) of a petal or an active role for the midribs (4, 5). However many flower petals have rippled edges, and this raises another qualitatively different possibility that we will explore here, namely that it is possible to change the shape of a lamina via excess growth of the margins relative to the center. This mechanism of differential planar growth has recently been shown to both explain the morphology of saddle and ripple shaped leaves and algal blades (6–10) and to engineer the shape soft thin sheets using differential swelling (11). Indeed, our approach quantifies and synthesizes the observations of von Goethe (12) who argued that flower petals are analogous to leaves physiologically.

Observations and Experiments

We study the process of blooming in the common lily *Lilium casablanca* as its popularity and large size makes it easily available and amenable to manipulation. Anatomically, a lily bud consists of 3 inner petals embraced by 3 outer sepals shown in Fig. 1 *A* and *B*. All petals/sepals are convex doubly curved surfaces (i.e., they are curved simultaneously in two orthogonal directions at all points along the mid surface), with their longitudinal curvature less than their lateral curvature. Both petal and sepals have midribs that are bilayer composite structures (Fig. 2*A*) with a soft leafy part (gray) that is contiguous with the petal/sepal and a stiff woody part (green) that is distinct from the lamina. Whereas the midrib of the outer sepals are featureless, those of the inner petals have grooves into which the margin of the outer sepals are tucked, as shown in Fig. 1*A*. This locking mechanism maintains the structural integrity of the bud while allowing for the rapid deployment of the petals once blooming starts.

To follow the bud of the Lily *Lilium casablanca*, we place it with its stem immersed in water in an environment of uniform humidity and temperature, under continuous fluorescent lighting and then film it with time lapse video to record the blooming process at intervals of 1 min. The blooming process takes four and a half days until the lily opens fully over which time we ensure that the ambient conditions are kept constant (Movie S1). Fig. 1*C* shows a typical opening sequence of a lily. During the first 4 days, the young green bud (10 cm long and 2.5 cm wide) absorbs about 0.2 L of water, increasing in length by 10% and in diameter by 20% and turns white. Although the bud is closed at the end of this stage, it is ready to burst forth quite literally; evidence for this can be seen by peeling back the outer sepals that show that the inner petals have wrinkled edges, as shown in Fig. 2*C*. It is worth pointing out that the inner petals wrinkle before blooming whereas the outer sepals wrinkle at the end of blooming. At the end of the fourth day (Fig. 1*C* and Movie S1) these growth-induced stresses in the bud reach a critical value large enough to overcome the petal-sepal lock. This causes the flower to bloom rapidly as the petals/sepals reverse curvature and bend outward. Simultaneously, wrinkles of typical wavelength (approximately 1.5 cm) develop along the edges of these laminae. To quantify the growth of these tissues, we paint equidistant black dots (1-cm apart) along both the periphery, the center, and along the midribs of both the petal and sepal in their closed state and track them over time. This allows us to measure the total in-plane relative growth strain of the tissue along the long axis of the petal over the period associated with blooming. We find that there is a growth strain 10% of the midrib in both petals and sepals is relatively uniform. However, the marginal growth strain in the sepal in the longitudinal direction is more than 20% basally and increases to nearly 50% distally (Fig. 3*A*). This lateral strain gradient in a lamina of finite width can give rise to global saddle-shaped structures as well as rippled edges (10) and is consistent with our observations of wrinkling of the petal edges in the prestressed bud and in the fully bloomed lily. In addition to

Author contributions: H.L. and L.M. designed research, performed research, analyzed data, and wrote the paper.

The authors declare no conflict of interest.

This article is a PNAS Direct Submission.

[1]To whom correspondence should be addressed. E-mail: lm@seas.harvard.edu.

This article contains supporting information online at www.pnas.org/lookup/suppl/doi:10.1073/pnas.1007808108/-/DCSupplemental.

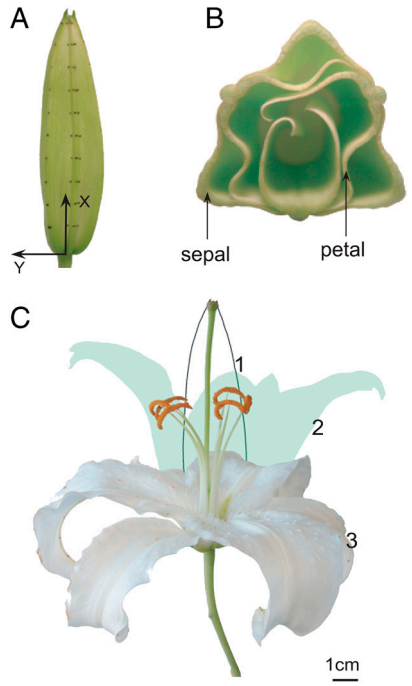

Fig. 1. Observations of and experiments on blooming in the asiatic lily *Lilium casablanca*. (*A*) A young green lily bud. The black dots separated by 1 cm allow us to measure growth strains. (*B*) The cross-section of a lily bud. (*C*) A typical opening sequence of a lily flower over a period of 4.5 days. The black line is the profile in the bud state, the transparently light blue shows the half-open state, and the white one is the fully open state.

the longitudinal growth, we also observe a 7% increase in the width of petals/sepals, that leads to a circumferential hoop stress on the bud.

Previous investigators have implicated the midrib as being crucial in the mechanism of blooming (4, 5). Indeed, the midrib is woodier than the lamina, but measurements of the stiffness of

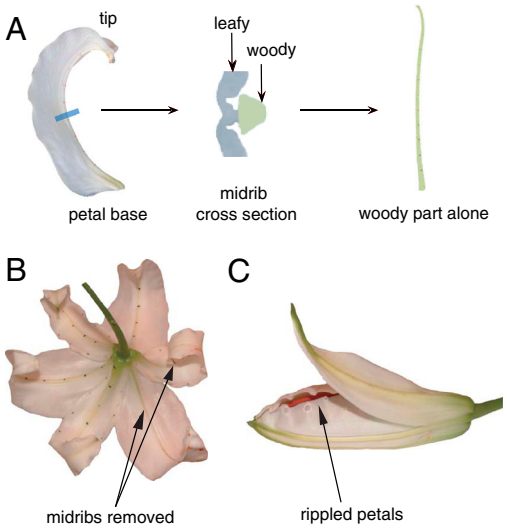

Fig. 2. Anatomy of the lily bud and the role of midrib. (*A*) The composite structure of a petal midrib: the *Left* panel shows a single petal; the *Center* panel shows the grooved structure of the midrib; the *Right* panel shows that when the leafy part (gray) is peeled away, the woody part straightens out, a sign that there is some relative growth between the two. (*B*) When the midribs are removed from a petal and a sepal, the flower can still bloom normally, with a slightly different curvature relative to the pristine petals/sepals. (*C*) The inner petals have rippled edges in the bud, showing clearly that their edges are growing relative to the rest of the tissue.

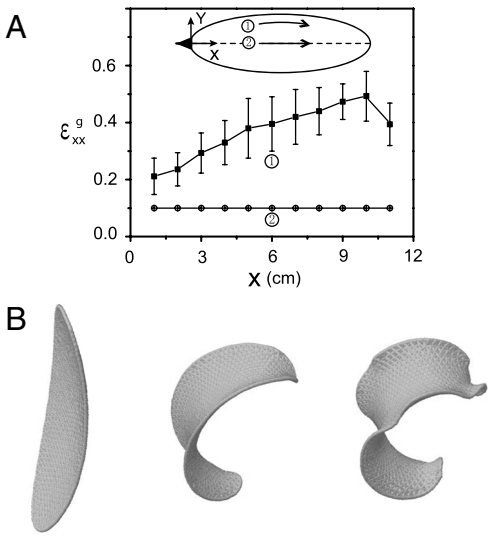

Fig. 3. Experimental measurement of differential growth and numerical simulation in a single petal. (*A*) Longitudinal growth strain ε_{xx}^{g} along the midrib and the edges varies in the lateral (*y*) direction. The edge growth strain is averaged over 6 sepals, and the midrib growth strain is averaged over 10 petals/sepals. This lateral growth gradient is sufficient to drive blooming. (*B*) Simulation of the blooming process in a single elliptical petal that is originally a convex spherical shell. As the edge-growth strain increases (see text for details), the curvature of the petal first reverses; i.e., it blooms. and then edge-localized ripples arise. The order of blooming and rippling can be reversed by changing the relative distribution of growth strains as can be seen in the inner and outer petals and sepals that follow opposite paths.

the midrib and the lamina (*SI Text*) shows that the leafy part accounts for 78% and the woody part accounts for 22% of the total bending stiffness of a shell-like petal; the curvature of the lamina and its width more than making up for the difference in the actual Young's modulus between the woody and leafy parts of a petal. To find whether midrib is essential for blooming or not, we shaved the midrib from one sepal and a petal when a lily is a bud, and find that both the sepal and the petal without the midrib open normally just like the other petals/sepals; the small difference in the final curvature is because the stiffness of the midrib composite is different from that of the petal/sepal. To further quantify the role of the midrib in flower opening, we shaved it from a fully bloomed lily and then peeled away the woody part from the petal (Fig. 2*A*). We find that the leafy part is about 4.5% (averaged over 10 samples) longer than the woody part and induces a spontaneous outward curvature that enhances flower opening. These observations show unequivocally that the midrib is neither necessary nor dominant in driving blooming.

Another possibility for the underlying mechanism behind blooming is the generation of spontaneous curvature due to differential growth of the inner (adaxial) surface of the petal/sepal relative to the outer (abaxial) one. Earlier experimental evidence (5) shows that cell size on both surfaces of a petal is the same at the onset of blooming and further that there is no cell proliferation, suggesting that differential growth of the adaxial and abaxial surface is not likely to play any role in blooming. To corroborate this on the organ scale, we note that surface differential growth will cause a shell-like petal will bend outward more if marginal tissues are removed, because the cross-section of a petal becomes less curved and the longitudinal bending stiffness decreases dramatically. However, we see both petals/sepals become less curved when the lateral edges of the petals are cut away (Figs. S1 and S2), which contradicts the hypothesis that relative surface expansion drives blooming.

Finally, we observe a slight rotation of the base of the petal/sepal relative to the flower axis consistent with earlier

observations (5). However, this cannot and does not lead to the reversal of curvature in the petals and is thus responsible only for a small contribution to the final conformation of the flower. Taken together these observations, combined with the edge rippling of petals that is observed both in the bud and bloomed states clearly shows that edge growth is both necessary and sufficient for blooming, and hereuntofore we will focus on understanding how this is brought about.

Mathematical Model of Blooming

At a mesoscopic scale, because both cell elongation and cell proliferation lead to differential growth and strain, we see that the mechanical basis for the margin-driven deployment of a doubly curved petal stems from the coupling between bending and stretching in thin curved shells. A minimal theory that couples growth to the shape of a thin lamina of nonuniform thickness takes the form of the Föppl–von Kármán equations (13) generalized to account for differential growth, both in the plane and across the thickness (10), as well as a nonzero natural curvature of the shallow shell. These may be written as

$$\Delta\left(\frac{\Delta\Phi}{t}\right)-(1+\nu)\left[\frac{1}{t},\Phi\right]+\frac{E}{2}([w,w]-[w_0,w_0])+E\lambda_g=0 \quad [1]$$

$$\Delta(D\Delta(w-w_0))-(1-\nu)[D,w-w_0]-[\Phi,w]+\Omega_g=0, \quad [2]$$

where $\partial_{xy}P=\partial^2P/\partial x\partial y$, $\Delta P=\partial_{xx}P+\partial_{yy}P$, $[P,Q]=\partial_{xx}P\partial_{yy}Q-2\partial_{xy}P\partial_{xy}Q+\partial_{xx}Q\partial_{yy}P$, $t(x,y)$ is the spatially inhomogeneous thickness, ν is Poisson's ratio, E is Young's modulus, $D=Et^3/12(1-\nu^2)$ is the bending stiffness of the shell that is assumed to be made of a linear isotropic material, Φ is the Airy stress potential, $w_0(x,y)$ is the initial transverse coordinate, and $w(x,y)$ is the current coordinate. The in-plane differential growth tensor is

$$\lambda_g=\partial_{yy}\epsilon^g_{xx}+\partial_{xx}\epsilon^g_{yy}-2\partial_{xy}\epsilon^g_{xy}, \quad [3]$$

while the differential growth gradient across the thickness leads to a transverse curvature growth tensor

$$\Omega_g=\partial_{xx}[D(\kappa^g_{xx}+\nu\kappa^g_{yy})]+\partial_{yy}[D(\kappa^g_{yy}+\nu\kappa^g_{xx})]+2(1-\nu)\partial_{xy}(D\kappa^g_{xy}), \quad [4]$$

which is the equivalent pressure induced by transverse growth gradients. Eq. **1** quantifies the incompatibility of the in-plane strain due to (*i*) the difference in the Gauss curvature $[w,w]$ of the shell (an intrinsic invariant of the surface) from its natural value $[w_0,w_0]$ and (*ii*) the additional contribution from in-plane differential growth. Eq. **2** describes the force balance in the out-of-plane direction due to the in-plane stresses in the curved shell and the growth curvature tensor associated with transverse gradients in the growth. In light of our experimentally measured growth strains shown in Fig. 3*A* we retain only the term $\partial_{yy}\epsilon^g_{xx}$, ignoring all other components of the in-plane growth strain tensor and the transverse growth curvature tensor entirely, given that our experiments eliminate the role of the midrib as the primary driver of blooming,

To complete the formulation of the problem, we prescribe the boundary conditions that the edge Γ of the shallow elliptical shell is free of torques and forces, so that (13),

$$D\{\partial_{nn}+\nu(\partial_{ss}+\partial_s\psi\partial_n)\}(w-w_0)|_\Gamma=0 \quad [5]$$

$$\{D[\partial_n\Delta+(1-\nu)\partial_s(\partial_{ns}-\partial_s\psi\partial_s)]+\partial_nD[\partial_{nn}+\nu(\partial_{ss}+\partial_s\psi\partial_n)]+2(1-\nu)\partial_sD[\partial_{ns}-\partial_s\psi\partial_s]\}(w-w_0)|_\Gamma=0, \quad [6]$$

where n is the unit normal and s is the arc length along the boundary curve Γ of the elliptical shell which has a curvature $\partial_s\psi$.

The nonlinear system of partial differential Eqs. **1–6** has no analytic solutions for general forms of the thickness and/or growth strain tensor, and so one must resort to approximate methods of solution. We use a combination of numerical method that allows us to explore the parameter regimes of the problem, and also show that a simple exact solution for a class of thicknesses and growth strains captures the essence of the mechanisms at play.

Analysis

Numerical Simulations. We follow (14) and use a discrete approximation to an elastic shell in terms of equilateral-triangular elements, with the elastic energy density $F=F_s+F_b$ as the sum of the stretching energy $F_s=\frac{\sqrt{3}S}{4}\Sigma_{ij}(r_{ij}-a_0)^2$, where r_{ij} is the current spring length and a_0 is the rest spring length and the bending energy $F_b=\frac{B}{\sqrt{3}}\Sigma_{\alpha\beta}(\vec{n}_\alpha-\vec{n}_\beta)^2$, where $\vec{n}_\alpha$ and $\vec{n}_\beta$ are the unit normal vectors of the two facets, and S and B are the 2D Young's modulus and bending stiffness respectively. In the continuum limit as $a_0\to 0$, the total discrete energy density F_s+F_b converges to the continuum elastic energy density of a shell

$$F=\frac{1}{2}\iint\left(\frac{Eh^3}{12(1-\nu^2)}F_b+\frac{Eh}{1-\nu^2}F_s\right)dxdy, \quad [7]$$

where the bending energy density $F_b=(\partial_{xx}w^e+\partial_{yy}w^e)^2+2(1-\nu)[(\partial_{xy}w^e)^2-\partial_{xx}w^e\partial_{yy}w^e]$ with $\partial_{ij}w^e=\partial_{ij}(w-w_0)-\kappa^g_{ij}$ and the stretching energy density $F_s=(\epsilon^e_{xx}+\epsilon^e_{yy})^2+2(1-\nu)(\epsilon^{e2}_{xy}-\epsilon^e_{xx}\epsilon^e_{yy})$ with $\epsilon^e_{ij}=\epsilon_{ij}-\epsilon^g_{ij}$. The Euler–Lagrange equations associated with the functional in Eq. **7** yield Eqs. **1** and **2**.

Minimizing the discrete energy given above as a function of the relative in-plane growth strain, characterized in terms of the variations in the rest length a, allows us to simulate the deployment of the petal/sepal. Scaling all lengths by the thickness of the petal ($h=1$ mm), we generate an elliptical shallow shell of semimajor axis $a=25$ (longitudinal axis x) and semiminor axis $b=10$ (lateral axis y) with natural curvatures $\kappa_x=0.04$ and $\kappa_y=0.02$. To mimic the differential growth gradients in the petal, we increase the rest length of the springs using the form $\epsilon^g_{xx}=(y/b)^4+e^{-(b-y)}$; the first term generates the global saddle shape whereas the second is responsible for edge rippling, simulating the behavior of outer sepals. To minimize the discrete analog of Eq. **7**, we use a damped molecular dynamics method (15) with a series of incremental growth strains of 0.01% followed by 100,000 steps with time step $\Delta t=0.1$ until equilibrium is reached. The results are shown in Fig. 3*B*, and as a movie (Movie S2), and clearly show both the blooming process as well as the subsequent wrinkling of the edge. Variations in lateral growth gradients can lead to a reversal of the sequence of the event such that edge rippling precedes global curvature change.

Whereas our numerical simulations allow us to probe the effect of strong edge-localized lateral growth gradients in an elliptical doubly curved elastic shell and are consistent with experimental observations, they do not expose the underlying simplicity of the mechanisms involved. This can be seen using an analytic theory, which we turn to next.

Simplified Theory. We focus on the consequence of minimal quadratic gradient in the growth strain that yields an exactly solvable theory of blooming, analogous to that thermally induced buckling in shells (13). It is sufficient to consider a single petal, modeled as a shallow elliptical shell of semimajor axis a (longitudinal axis x) and semiminor axis b (lateral axis y) with a naturally convex shape, as shown in Fig. 4*A*. We describe its transverse coordinate using $w_0=-\frac{1}{2}(\kappa_{x0}x^2+\kappa_{y0}y^2)$ with $\kappa_{x0}>0$ and $\kappa_{y0}>0$ the

spontaneous principal curvatures. For convenience, we define a dimensionless parameter $m = \kappa_{x0}/\kappa_{y0}$ to characterize the shape of the natural curved petals; for most petals $m \in [0,1]$, so that they are weakly curved longitudinally and strongly curved laterally. Following our observations and measurement on lily petals and sepals, we assume that the dominant contribution to the growth is given by $\epsilon^g_{xx} = g(y/b)^2$ with $g > 0$ denoting the maximum value at the edge, and $\epsilon^g_{yy} = \epsilon^g_{xy} = 0$. The current transverse coordinate takes the form of $w = -\frac{1}{2}(\kappa_x x^2 + \kappa_y y^2)$ with κ_x and κ_y the principal curvatures of the deformed shape. Finally, we assume that a petal may be modeled as a shell with a lenticular cross-sections (i.e., a thickness $t = t_0(1 - \frac{x^2}{a^2} - \frac{y^2}{b^2})$) where t_0 is the maximum thickness of the shell at its center, so that its bending rigidity is

$$D = D_0\left(1 - \frac{x^2}{a^2} - \frac{y^2}{b^2}\right)^3, \qquad [8]$$

where $D_0 = Et_0^3/12(1-\nu^2)$. Then, if the Airy stress potential

$$\Phi = \beta D(x,y) \qquad [9]$$

with β an unknown constant that describes the in-plane elastic response, we find that along the boundary Γ of the elliptical shell

$$D|_\Gamma = \partial_n D|_\Gamma = \Phi|_\Gamma = \partial_n \Phi|_\Gamma = 0 \qquad [10]$$

vanish identically so that the boundary conditions Eqs. **5** and **6** are also satisfied identically. The assumption of a lenticular cross-section with a thickness that varies quadratically (at least) is tantamount to stating that the forces and torques on the edges vanish faster than either the in-plane stress or the curvature, so that the edges are automatically free of forces and torques (13).

The above assumption of a quadratic form for the lenticular cross-section, the original and the current displacement field and the growth strain allows us to reduce Eqs. **1** and **2** to a set of three nonlinear algebraic equations (13)

$$\bar\kappa_x\bar\kappa_y - \bar\kappa_{x0}\bar\kappa_{y0} = -\beta - \beta_g \qquad [11]$$

$$(1+\nu-\beta)(\bar\kappa_x + \bar\kappa_y) = (1+\nu)(\bar\kappa_{x0} + \bar\kappa_{y0}) \qquad [12]$$

$$(1-\nu+\beta)(\bar\kappa_x - \bar\kappa_y) = (1-\nu)(\bar\kappa_{x0} - \bar\kappa_{y0}), \qquad [13]$$

with three dimensionless unknowns β, $\bar\kappa_x$, and $\bar\kappa_y$. Here, $\beta_g = 2g/\bar b^2$ is a measure of growth strain, β is a measure of the elastic in-plane strain as characterized by (9), $\bar\kappa_{x0} = \kappa_{x0}L$, $\bar\kappa_{y0} = \kappa_{y0}L$, $\bar\kappa_x = \kappa_x L$, $\bar\kappa_y = \kappa_y L$, and $\bar b = b/L$, with the intrinsic length $L = \frac{ab}{t_0}\left(\frac{1-\nu^2}{4+2\nu+5(a^2/b^2+b^2/a^2)}\right)^{1/2} \equiv \lambda^{1/2}ab/t_0$. It is useful to introduce a parameter $\alpha = \bar\kappa_{x0}\bar\kappa_{y0} = m\bar\kappa_{y0}^2$, a rescaled natural Gauss curvature that measures the bend-stretch coupling, so that there is a critical growth strain $\beta_g^* = \beta_g^*(\bar\kappa_{x0},\bar\kappa_{y0})$ that demarcates the stretch-dominated regime from the bend-dominated regime.

To see how a petal changes its geometry during blooming, we first explore the case of naturally curved spherical shell with $\bar\kappa_{x0} = \bar\kappa_{y0} = \bar\kappa_0 > 0$ (or $m = 1$), so that Eqs. **11–13** read

$$\bar\kappa_x\bar\kappa_y - \bar\kappa_0^2 = -\beta - \beta_g \qquad [14]$$

$$(1+\nu-\beta)(\bar\kappa_x + \bar\kappa_y) = 2(1+\nu)\bar\kappa_0 \qquad [15]$$

$$(1-\nu+\beta)(\bar\kappa_x - \bar\kappa_y) = 0. \qquad [16]$$

The above equations have two solution regimes depending on the magnitude of the differential growth β_g relative to a critical value $\beta_g^*(\kappa_0,\kappa_0) = (1-\nu) + \frac{1}{4}(1-\nu)(3+\nu)\bar\kappa_0^2$ as for thermally induced buckling (13).

(*i*) *Before buckling*: $0 < \beta_g < \beta_g^*$. From Eq. **16**, we see that if $1 - \nu + \beta \neq 0$, then $\bar\kappa_x = \bar\kappa_y$, and the first two Eqs. **14** and **15** yield the cubic

$$(\bar\kappa_x - \bar\kappa_0)\{\bar\kappa_x(\bar\kappa_x + \bar\kappa_0) + 1 + \nu\} + \beta_g\bar\kappa_x = 0, \qquad [17]$$

with only one real root for $\bar\kappa_x$, and furthermore

$$\beta = (1+\nu)\left(1 - \frac{\bar\kappa_0}{\bar\kappa_x}\right). \qquad [18]$$

Thus we see that as the growth strain β_g increases from zero, the shell unbends slowly but remains spherical, while the in-plane strain β decreases monotonically as shown in Fig. 4*C*.

(*ii*) *After buckling*: $\beta_g \geq \beta_g^*(\bar\kappa_0,\bar\kappa_0) > 0$. Now the curvatures are unequal after buckling (i.e., $\bar\kappa_x \neq \bar\kappa_y$), so that third of Eq. **16** requires $\beta = \nu - 1$. Then we may solve for the curvatures from Eqs. **14** and **15** to get

$$\bar\kappa_x = \frac{1+\nu}{2}\bar\kappa_0 - (\beta_g - \beta_g^*)^{1/2} \qquad [19]$$

$$\bar\kappa_y = \frac{1+\nu}{2}\bar\kappa_0 + (\beta_g - \beta_g^*)^{1/2}; \qquad [20]$$

i.e., there is a pitchfork bifurcation in the solution and the shell suddenly unbends anisotropically with the petal bending outward longitudinally while curving inward laterally. Fig. 4*B* shows three typical configurations of a shell with an elliptical planform cut from a spherical cap as it opens. We pause to observe that when $\beta_g > \beta_g^*$, the stretching strain $\beta = \nu - 1$ becomes constant, indicating the exchange of stability from a stretch-dominated regime to a bend-dominated regime of the shell occurs via pitchfork bifurcation as shown in Fig. 4*D*. Any further in-plane growth is converted directly to bending deformations, so that the shell becomes a perfectly efficient bending actuator beyond the bifurcation. The subsequent increase in longitudinal curvature is consistent with earlier observations (5), as well as our own.

More generally, when a petal is not spherically curved, $0 < \bar\kappa_{x0} < \bar\kappa_{y0}$ (or $m < 1$), the in-plane response characterized by β must be found by solving a quintic defined by Eqs. **11–13**

$$(1+\nu-\beta)^2[4(1-\nu+\beta)^2(\bar\kappa_{x0}\bar\kappa_{y0} - \beta - \beta_0) + (1-\nu)^2(\bar\kappa_{x0} - \bar\kappa_{y0})^2] - (1-\nu+\beta)^2(1+\nu)^2(\bar\kappa_{x0} + \bar\kappa_{y0})^2 = 0, \qquad [21]$$

using, for example, the polynomial root solver *FindRoot* in *Mathematica* (Fig. 4*D*). Again the shape of the petal as a function of the growth strain (i.e., $\bar\kappa_x$ and $\bar\kappa_y$) is obtained from Eqs. **12** and **13** as shown in Fig. 4*D*. We see that for nonspherical petals when $m < 1$, the pitchfork bifurcation is unfolded so that there is no sudden transition and the petal opens smoothly. However, there is still a critical value of the growth strain $\beta_g^*(\bar\kappa_{x0},\bar\kappa_{y0})$ that separates the stretch-dominated and bend-dominated regimes. In terms of the total elastic energy of the petal (see Eq. **7**) and its discrete analog, the critical point β_g^* is found when $\partial_{\beta_g}\partial_{\beta_g}F_s$ reaches a maximum, which $\partial_{\beta_g}\partial_{\beta_g}F_s$ signifies a switch from stretch-dominated deformations to bend-dominated deformations just as for a spherical curved shell with $m = 1$, as shown in Fig. 4*E*. Indeed, this transition may be quantified in terms of the stretch-bend geometric coupling parameter $\alpha = \bar\kappa_{x0}\bar\kappa_{y0} = m\bar\kappa_{y0}^2 \sim \Delta_{x0}\Delta_{y0}/t_0^2$ where $\Delta_{x0} = \lambda^{1/2}a^2\kappa_{x0}$ and $\Delta_{y0} = \lambda^{1/2}b^2\kappa_{y0}$ are the longitudinal and lateral rise respectively (16). In Fig. 4*E*, we see that when $\alpha \ll 1$, the critical scaled growth strain β_g^* is small, whereas when $\alpha > 1$, the critical growth strain β^* is large (i.e., a weakly curved

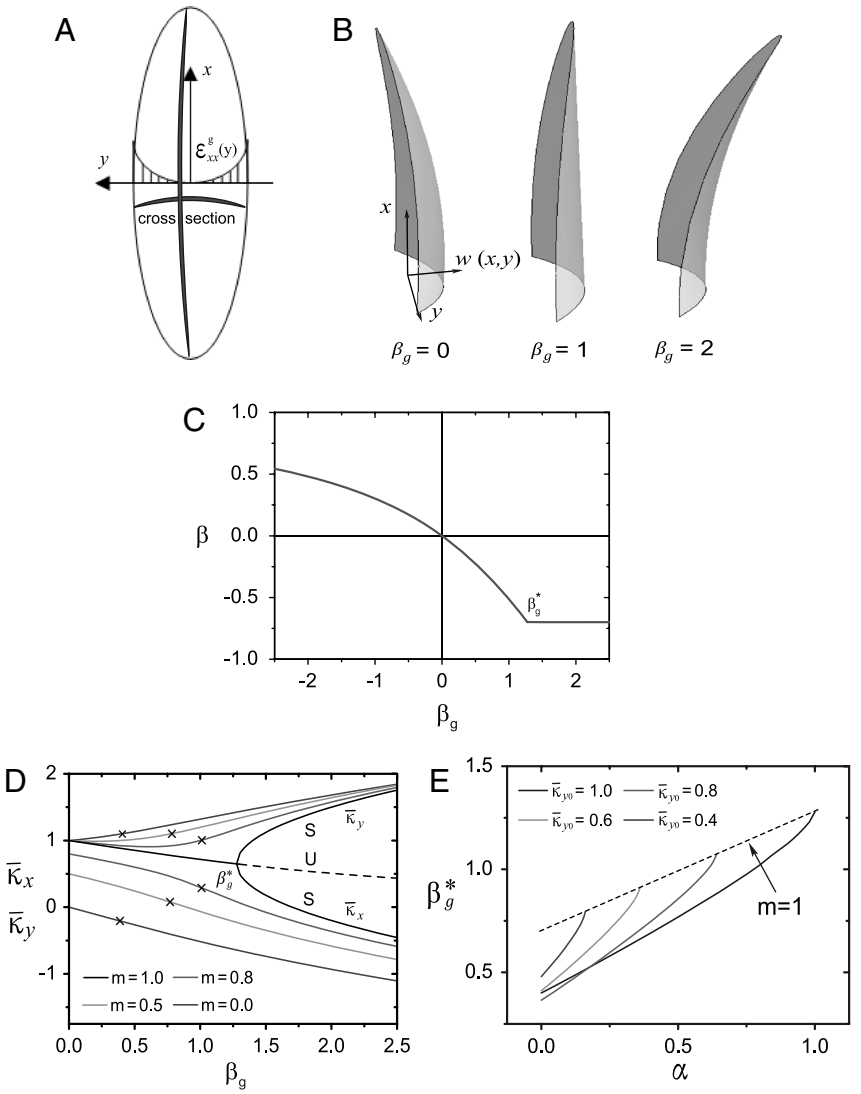

Fig. 4. A simple theory for the reversal of an elliptical shell. (*A*) A parabolic lateral growth strain ε^g_{xx} is prescribed on an elliptical concave shell with a lenticular cross-section along both the *x* and *y* axes and quadratically varying thickness (see text). (*B*) As the differential growth β_g increases from left to right, the shell reverses curvature; i.e., it blooms. (*C*) For an initially spherical shell with $\bar{\kappa}_{x0} = \bar{\kappa}_{y0} = \bar{\kappa}_0 = 1$, the elastic strain β as function of β_g has the signature of a pitchfork bifurcation. (*D*) The rescaled curvatures $\bar{\kappa}_x$ and $\bar{\kappa}_y$ as function of growth strain β_g, and $\bar{\kappa}_{y0} = 1$. (Notation: S-stable, U-unstable). (*E*) The critical point β^*_g denoting the transition from stretch-dominated to bend-dominated [denoted by × in (*D*)] as a function of the bend-stretch coupling parameter α for different $\bar{\kappa}_{y0}$, and the dotted line follows the analytic solution for the spherical case with $m = 1$. The parameters are chosen to correspond to the dimensions of a typical lily petal: $a = 3$, $b = 1$, $t_0 = 0.1$, $\nu = 0.3$.

petal will open when the growth strain is quite small, or equivalently, for a given growth strain rate associated with lateral gradients, a highly curved petal will open more slowly) a simple testable prediction of our theory.

Discussion

Our observations, experiments, theory, and simulation show that the dynamic deployment of petals during blooming is an edge-driven morphological transition in a curved lamina, thus illuminating Goethe's analogy between leaves and flowers (12) using physics, with an important qualitative difference, namely that flower petals are almost always naturally curved, unlike leaves. This example of functionally driven convergent evolution also has implications beyond biology. In addition to infusing a scientific aesthetic into a thing of beauty, our study suggests a biomimetically inspired approach to thin film morphologies that may be controlled by edge actuation rather than surface actuation, with some similarities to engineer the shape of elastic sheets using a tunable metric (11) but here emphasizing the role of the boundary in controlling the behavior in the interior, and easily adapting as a design tool for a new generation of bimorphs.

ACKNOWLEDGMENTS. We thank the Harvard–National Science Foundation Materials and Research Science and Engineering Center and Defense Advanced Research Projects Agency for partial financial support.

1. Higgins M, Pramer D (1967) Fungal morphogenesis: Ring formation and closure in arthrobotrys dactyloides. *Science* 155:345–46.
2. Forterre Y, Skotheim JM, Dumais J, Mahadevan L (2005) How the Venus flytrap snaps. *Nature* 433:421–425.
3. Skotheim JM, Mahadevan L (2005) Physical limits and design principles for plant and fungal movements. *Science* 308:1308–1310.
4. van Doorn WG, van Meeteren U (2003) Flower opening and closure: A review. *J Exp Bot* 54:1801–1812.
5. Bieleski R, Elgar J, Heyes J (2000) Mechanical aspects of rapid flower opening in the Asiatic Lily. *Ann Bot* 86:1175–1183.
6. Nath U, Crawford BCW, Carpenter R, Coen E (2003) Genetic control of surface curvature. *Science* 299:1404–1407.

7. Sharon E, Marder M, Swinney HL (2004) Leaves, flowers, and garbage bags: Making waves. *Am Sci* 92:254–261.
8. Dervaux J, Ben Amar M (2008) Morphogenesis of growing soft tissues. *Phys Rev Lett* 101:068101–068104.
9. Koehl M, Silk W, Liang H, Mahadevan L (2008) How kelp produce blade shapes suited to different flow regimes: A new wrinkle. *Integr Comp Biol* 48:834–851.
10. Liang HY, Mahadevan L (2009) The shape of a long leaf. *Proc Natl Acad Sci USA* 106:22049–55.
11. Klein Y, Efrati E, Sharon E (2007) Shaping of elastic sheets by prescription of non-euclidean metrics. *Science* 315:1116–1120.
12. von Goethe JW (1790) *Metamorphosis of Plants* (MIT Press, Cambridge, MA), (translated from German).
13. Mansfield EH (1989) *The Bending and Stretching of Plates* (Cambridge University Press, Cambridge, UK), 2nd Ed.
14. Seung HS, Nelson DR (1988) Defects in flexible membranes with crystalline order. *Phys Rev A* 38:1005–1018.
15. Allen MP, Tildesley DJ (1987) *Computer Simulation of Liquids* (Clarendon, Oxford).
16. Timoshenko SP, Gere JM (1985) *Theory of Elastic Stability* (McGraw-Hill, New York).

Supplementary Information for "How the Lily Blooms"

Haiyi Liang[1] & L. Mahadevan[1,2]

Engineering and Applied Sciences, Harvard University, Cambridge, MA 02138, USA

Organismic and Evolutionary Biology, Harvard Medical School, Boston, MA 02115, USA

I. THE RELATIVE ROLE OF EDGE ACTUATION

Having demonstrated that the midrib is unnecessary for the actuation of the blooming response (Fig.2, main text), we now focus on the role of edge actuation on blooming by considering the morphology of the petal/sepal (without midribs) both before and after the edges have been surgically removed. In Fig.S1, we show the results of these experiments. We can see that sepal/petal whose edge is cut opens out and exhibits a smaller curvature compared to those with intact edges, as viewed from two perspectives. In Fig.S1, the average radius of curvature of the intact petal is $\sim 2cm$ while that of the one with edges removed is $\sim 5cm$. We see that there is a variation of the curvature as a function of location along the longitudinal axis of the petal; in particular removing the edges causes the petal to spring back near the apex much more than near the base. This is because edge actuation is far more dominant where the petal-midrib composite is thinner (and less stiff), i.e. near the apex.

Thus, we see that the dominant mechanism underlying the blooming of a lily is that of edge actuation of a thin lamina. Of course there are quantitative corrections to this due to the presence of a midrib of thickness that varies along the longitudinal axis and a hinge -like actuation at the base itself, but the qualitative feature of curvature change induced by lateral growth persists, as evidenced by our surgical and mechanical measurements.

II. THE RELATIVE CONTRIBUTION OF THE LEAFY AND WOODY PARTS OF THE PETAL TO ITS STIFFNESS

In cross-section, a petal can be seen to be made of a woody midrib and a leafy tissue that forms the petal itself, as shown in Fig.S2. The leafy region has a thickness $t = 0.5mm$ and a midrib of diameter $d = 2mm$, and the cross section of a petal may be geometrically approximated by a half circle at the onset of opening, with a radius $r = 10mm$. To assess

FIG. S1: The shape of petals with and without its lateral edges. Midribs of both petals have been removed. (a) and (c) show the same petal with edge intact from two different perspectives, while (b) and (d) show the same petal with the edge removed from the same two perspectives. We see that near the apex, the curvature of the petal with intact edges is much larger than that of the petal with its edges removed. Near the base, the curvature of the petal with and without its lateral edges is similar because the thickness of the leafy and woody parts and thus the stiffness of the petal is so large that edge actuation alone is not enough.

the contributions of the two materials to the stiffness of the whole petal, we measured the Young's modulus of the leafy part E_l and woody parts of the midrib E_m using a microtensile tester (CMT80202 dual column electromechanical universal testing machine, MTS Systems Co.), after these regions were surgically separated from the leaf. We find that $E_l = 5$ MPa and $E_m = 20$ MPa. Similar measurement on herbaceous plants shows that the Young's modulus of parenchyma (leafy) and the sclerfied (woody) tissues are around 10^2MPa and $10^3 \sim 10^4$MPa [1]. The neutral axis of the composite is given by the expression

$$\overline{y} = \frac{\int_0^\pi r^2 t \sin\theta d\theta + A_m r}{\pi r t + A_m} = 8.0mm \tag{S.1}$$

where the effective area of midrib is $A_m = (E_m/E_l)\pi d^2/4 = 12.6mm^2$. The bending stiffness of leafy part is

$$B_l = E_l \int_0^\pi (r\sin\theta - \overline{y})^2 t r d\theta = 948.7Nmm^2 \tag{S.2}$$

The bending stiffness of midrib is

$$B_m = E_m[\frac{\pi d^4}{64} + A_m(r - \overline{y})^2] = 271.7Nmm^2 \tag{S.3}$$

Therefore, the contributions of leafy part and midrib to the total bending stiffness are 78% and 22% respectively, so that to a first approximation, we may neglect the effect of the midrib in determining the stiffness of the petal.

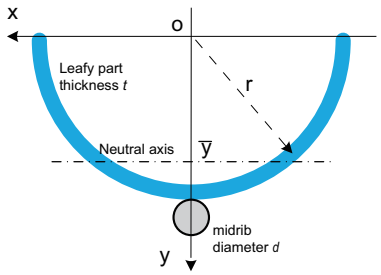

FIG. S2: The geometry of petal/sepal. The leafy part is well approximated by a semi-circle of radius r over much of its length, and the midrib is well approximated by a circle of diameter d.

---

[1] Moulia B, Fournier M. (1997) Mechanics of the maize leaf: a composite beam model of the midrib.*Journal of Materials Science,* **32**, 2771-2780.